JOURNAL OF SOLID STATE CHEMISTRY 86, 238–248 (1990)

X-Ray Absorption Study of Lithium Intercalated Thiophosphate $NiPS_3$

G. OUVRARD,[1] E. PROUZET, AND R. BREC

Laboratoire de Chimie des Solides, I.P.C.M., 2 rue de la Houssinière, 44072 Nantes Cedex 03, France

AND S. BENAZETH* AND H. DEXPERT

*LURE, Batiment 209D, Université de Paris-Sud, 91405 Orsay Cedex, France and *Laboratoire de Chimie Minérale Structurale, Université Paris V—75270 Paris Cedex 06, France*

Received October 9, 1989; in revised form February 5, 1990

An EXAFS study of lithium-intercalated $NiPS_3$ has been performed at the nickel K edge for various lithium contents. The large modifications of EXAFS spectra in the intercalates can be related to the displacement of reduced nickel atoms from their initial octahedral sulfur sites to tetrahedral ones within the slab. The results are discussed in comparison with previous physical measurements. Hypotheses for the reduction process and the induced structural modifications are proposed.

I. Introduction

The lamellar thiophosphates MPS_3 (M: transition metal in oxidation state II) can be considered as substituted disulfides TS_2 in which one third of the transition metal atoms is replaced by phosphorus–phosphorus pairs in octahedral sulfur sites (*1*). Like the well-known lamellar disulfide TiS_2, some MPS_3 compounds, especially $NiPS_3$ and $FePS_3$, have been extensively studied during the last 10 years for their ability to reversibly interacalate lithium (*2–4*). However, if we consider this intercalation, the thiophosphate behavior is very different from that of TiS_2. In effect, no noticeable modification of X-ray powder diffraction patterns has been observed in lithium-intercalated phases Li_xMPS_3 for $x < 1.5$, whereas TiS_2 shows continuous parameter variations corresponding to a cell volume expansion. Structural considerations could explain the absence of expansion of the van der Waals gap due to its initial large size (*5*). Because the transition metal has such a low oxidation state, many experiments have been performed in order to determine the redox center in the thiophosphates. ^{31}P NMR (*6*) and ^{57}Fe Mossbauer (*7*) spectroscopies have shown that the transition metal atom is reduced at the oxidation state zero, when MPS_3 (M = Fe, Ni) intercalates lithium which has been confirmed by the band structure calculations (*8*). This intercalation follows a microbiphased process. The reduction of the

[1] To whom correspondence should be addressed.

0022-4596/90 $3.00

transition metal must necessarily be accompanied by a local expansion of the sites related to the size increase of this cation. In order to observe the local structural modifications induced by lithium intercalation in the MPS_3 compounds (M = Ni and Fe), EXAFS experiments were performed at the transition metal K edge. This technique is well known to be powerful in observing such modifications and has already been used for the substituted–intercalated MPS_3 phases (*9, 10*). Preliminary results were briefly given in a previous paper (*11*). We describe here a complete and detailed study on lithium-intercalated phases of nickel thiophosphate and discuss the experimental results taking into account the previous physical results. A parallel study made on the iron derivatives will be published elsewhere.

II. Materials, Data Acquisition, and Analysis

Pure $NiPS_3$ has been obtained by heating the elements in stoichiometric proportions at 700°C in evacuated silica tubes. Using the butyllithium technique (*12*) $NiPS_3$ was intercalated as powders (diameter < 0.1 mm) at various compositions of Li_xNiPS_3 with $x = 0.30, 0.55, 0.90, 1.22$ and 1.49. The latter phase was deintercalated at the composition $Li_{0.37}NiPS_3$ using an iodine solution in acetonitrile and reintercalated at the composition $Li_{1.47}NiPS_3$ in order to observe the reversibility of the phenomenon. The lithium content was determined by atomic absorption spectroscopy. Because of their very high air sensitivity, the intercalated compounds had to be handled in an inert atmosphere. Due to this reactivity to moisture and in order to obtain a good and reproducible signal/noise ratio in the EXAFS experiments, the powders were mixed with dry boron nitride in suitable proportions (about 1/3 for $NiPS_3$/BN in weight) and put between two adhesive Kapton tapes in a void (5×30 mm^2) hollowed in a 1-mm-thick aluminum plate.

The X-ray absorption data of these powdered samples were recorded at room temperature at the nickel K edge between 8150 and 9150 eV using the synchrotron radiation emitted by the DCI storage ring at LURE. The monochromator was a Si (331) double crystal allowing harmonic rejection.

The EXAFS spectra were analyzed using a well-known procedure. The preedge absorption was fitted by a Victoreen expression extrapolated beyond the edge. The atomic absorption coefficient was approximated by a second degree polynomial expression and the remaining long wavelength oscillations removed by a multi-iteration curve smoothing. The Hanning window was applied to the $k^3\chi(k)$ weighted data before Fourier transforming extended from 50 to 700 eV. The origin of the energies E_0 was taken at half of the edge jump found at 8332 eV.

The backtransformed contribution of each of the various shells has been analyzed through the classical EXAFS formula, expressed with the notation

$$\chi(k) = -\sum_j \frac{N_j}{kR_j^2} \exp(-2\sigma_j^2 k^2) \cdot \exp(-2\gamma_j R_j/k) \cdot |f_j(\pi, k)| \sin(2kR_j + \phi_j)$$

with $\phi_j = 2\delta + \psi_j(k)$, where δ, ψ_j, and $|f_j(\pi, k)|$ are respectively the central atom phase shift and the phase and the amplitude of the backscattering atom, σ is the Debye–Waller-like factor, and γ is related to the mean free path of the photoelectron. In order to model the experimental spectra, we used theoretical amplitude and phase shifts obtained by Teo and Lee from ab initio calculations (*13*). σ and γ values were determined using the starting compound $NiPS_3$ as a model. Calculations performed on the first coordination shell using experimental amplitude and phase shifts extracted from the EXAFS of $NiPS_3$ gave very comparable results.

Previous structural determination performed by single crystal X-ray diffraction of $NiPS_3$ (*1b*) shows an octahedral sulfur coordination of nickel atoms wtih an average nickel–sulfur distance of 2.463(5) Å. The second coordination shell of nickel contains three nickel atoms at 3.357 Å and six phosphorus atoms at 3.524 Å.

III. Results

Figure 1 compares the moduli of the Fourier transforms of EXAFS spectra for the studied compositions in the Li_xNiPS_3 system. The first peak observed in $NiPS_3$ corresponds to the octahedral sulfur environment of nickel atoms. When lithium is intercalated, a new peak appears at a shorter distance. Its intensity increases with lithium content at the expense of the starting peak. At the same time the intensity of the second peak of $NiPS_3$ decreases regularly and moves to longer distance.

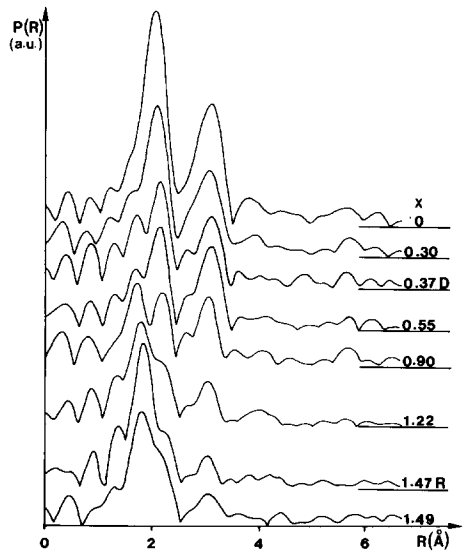

FIG. 1. Moduli of the Fourier transforms of the $k^3\chi(k)$ data at the Ni K edge for various compositions in the Li_xNiPS_3 system ($0 \leq x < 1.5$) (uncorrected for phase shift). D and R correspond respectively to the deintercalated and reintercalated phases.

A. Analysis of the First Coordination Shell

The occurrence of the short distance corresponding to the new peak in the Fourier transform moduli must be interpreted as a modification of the nickel environment, excluding an undesirable appearance of oxygen atoms to which correspond shorter bond distances of about 2 Å as found in the gel of amorphous $NiPS_3$ (*14*). The most probable hypothesis to consider is that of a migration of nickel atoms into tetrahedral sulfur sites. In effect the hypothesis of an off-centered position of the nickel atoms in the octahedral sites would correspond to the observation of a doublet at shorter and longer distances. Therefore the EXAFS spectra corresponding to the first coordination shell were fitted taking into account tetrahedral and octahedral sulfur environment for the nickel atoms. Values of γ and σ for octahedra were calculated from the known $NiPS_3$ to respectively 1.74 $Å^{-1}$ and 0.10 Å. A preliminary fit on the richer intercalated phase $Li_{1.49}NiPS_3$ gave the value of 0.10 Å for σ and a tetrahedral site. It is evident that the most important parameter variation in this case is the number of sulfur atoms corresponding to each type of site. Unfortunately, it is well known that this parameter is obtained by EXAFS with a rather low accuracy, usually between 10 and 20%. Furthermore, this value is strongly correlated with that of σ. In order to improve the accuracy and to obtain coherent results for all the series, we choose in the fits to keep σ at the above value (0.10 Å), γ being kept at 1.74 $Å^{-1}$.

The results obtained in these fits are summarized in the Table I and a comparison between experimental and calculated signals can be found on Fig. 2. The Ni–S distances $R1$ and $R2$ are fairly constant for all the series, in consistency with the previously observed microbiphased process. These values fit well, for the octahedral site

TABLE I

RESULTS OF THE FITS FOR THE FIRST NICKEL COORDINATION SHELL

x in Li$_x$NiPS$_3$	$N1$	$R1$(Å)	$N2$	$R2$(Å)	ΔE_0(eV)	r(%)	$X1$	$X2$
0.00	0.1	2.30	5.9	2.44	13.2	0.24	0.02	0.98
0.30	0.7	2.30	4.2	2.45	13.8	0.21	0.17	0.70
0.55	1.1	2.27	3.0	2.44	15.0	0.40	0.28	0.50
0.90	1.9	2.28	1.7	2.45	16.8	2.41	0.47	0.28
1.22	2.4	2.28	1.0	2.44	17.8	2.35	0.60	0.17
1.49	2.8	2.28	0.1	2.45	16.7	1.70	0.70	0.02
0.37 D	1.2	2.29	3.3	2.45	13.6	0.29	0.30	0.55
1.47 R	3.0	2.29	0.2	2.44	18.3	1.92	0.75	0.03

Note. N and R represent respectively the number of sulfur atoms and the Ni–S distances. 1 and 2 refer respectively to tetrahedral and octahedral environment. $X1$ and $X2$ are the fraction of nickel atoms in each type of site ($X1 = N1/4$ and $X2 = N2/6$). ΔE_0 and r represent the edge variation and the reliability factor of the fit.

(dNi–S_{Oh} = 2.45 Å) with the value calculated by X-ray structural determination (2.463 Å), and for the tetrahedral one (dNi–S_{Td} = 2.28 Å) with the value encountered for tetrahedral nickel coordination, as, for example, in Ta_2NiS_5 (2.25 Å) (*15*). The E_0 variation is small but quite regular and must correspond to the new coordination and oxidation state of nickel. As it is suggested by the variations observed on Fig. 1, the values of $N1$ which represents the number of sulfur atoms forming a tetrahedral coordination increase with x. At the same time $N2$, which corresponds to octahedra, decreases. In order to have a more realistic point of view, we have calculated the $X1$ and $X2$ values which represent the fraction of nickel atoms respectively in tetrahedral and octahedral sulfur environment, simply dividing $N1$ by four and $N2$ by six. We will discuss later the $X1 + X2$ values lower than 1.

B. Analysis of the Second Coordination Shell

If we consider the spectra on Fig. 1, the only noticeable modification of the second contributions which appear around 3 Å in the different moduli concerns the intensity, but neither the shape (no stretch of thin peak is observed) nor the position of the peak. Thus the fits were performed taking into account the nickel and phosphorus environment of the absorbing nickel atom. As above, the EXAFS spectrum of the starting compound $NiPS_3$ allowed us to determine the two values of σ and γ, respectively, 0.102 Å and 0.087 Å for σ_{Ni} and σ_P, and 1.705 Å^{-1} for γ. These terms were kept constant in the fits for all the series. Figure 2 contains an example of comparison between experimental and calculated signals. Table II summarizes the results of the fits obtained by varying the numbers of nickel and phosphorus atoms, the nickel–nickel and nickel–phosphorus distances, and the edge energy E_0. The values of the inter-

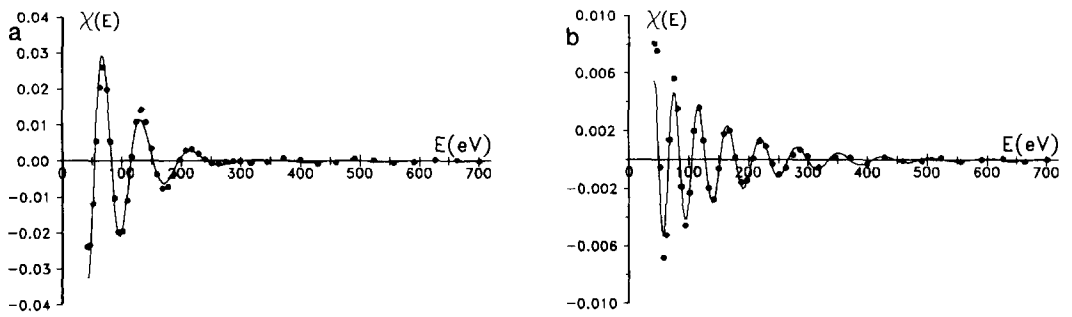

FIG. 2. Some fits between experimental (dots) and calculated (solid lines) signals at the nickel edge. (a) First coordination shell for $Li_{0.90}NiPS_3$. (b) Second coordination shell for $Li_{1.47}NiPS_3$ reintercalated phase.

TABLE II

RESULTS OF THE FITS FOR THE SECOND NICKEL COORDINATION SHELL

x in Li_xNiPS_3	N_{Ni}	$D1$(Å)	N_P	$D2$(Å)	ΔE_o(eV)	r(%)	$Y1$	$Y2$
0.00	3.0	3.29	6.1	3.53	4.6	0.18	1.00	1.02
0.30	2.5	3.29	4.5	3.54	4.2	0.22	0.83	0.75
0.55	1.6	3.29	4.2	3.53	4.3	0.40	0.53	0.70
0.90	1.3	3.28	3.1	3.52	2.1	0.80	0.43	0.52
1.22	0.6	3.28	2.5	3.52	2.0	0.96	0.20	0.42
1.49	0.5	3.27	2.0	3.54	3.9	0.43	0.17	0.33
0.37 D	1.2	3.27	4.2	3.53	2.4	0.29	0.40	0.70
1.47 R	0.2	3.28	1.9	3.53	1.9	2.07	0.07	0.32

Note. N_{Ni} and N_P represent the numbers of nickel and phosphorus atoms surrounding absorbing nickel. $D1$ and $D2$ are the Ni–Ni and Ni–P distances. $Y1$ and $Y2$ are the fractions of nickel atoms keeping the starting environment deduced respectively from N_{Ni} and N_P ($Y1 = N_{Ni}/3$ and $Y2 = N_P/6$). ΔE_o and r represent the edge variation and the reliability factor of the fit.

atomic distances do not vary in the series and are consistent with those obtained by X-ray diffraction (3.28 Å and 3.35 Å for Ni–Ni, 3.53 Å and 3.52 Å for Ni–P). As above, from the fitted numbers of nickel and phosphorus atoms, the fraction of nickel atoms keeping the pristine environment was calculated by dividing respectively N_{Ni} and N_P by three and six. The corresponding values $Y1$ and $Y2$ are gathered in Table II.

IV. Discussion

Successively we will consider the results obtained by EXAFS in terms of local structural modifications and, taking into account the previous results obtained by physical experiments on these intercalated phases, we will try to structurally describe the intercalation process.

A. Modification of the Close Nickel Environment

In Fig. 3, the values of $X1$ and $X2$ (Table I) corresponding to the fractions of nickel atoms respectively in tetrahedral and octahedral environments versus x in Li_xNiPS_3 are marked. They can be compared with two lines of slope $\frac{1}{2}$ (full line) and $-\frac{1}{2}$ (dotted line) representing the variations of the numbers of reduced and unreduced nickel atoms in the hypothetical intercalation reaction,

$$x\ Li + Ni^{II}PS_3 \rightarrow Li^{I}_x Ni^{0}_{x/2} Ni^{II}_{1-x/2} PS_3,$$

or, if we consider that the intercalation process is microscopically biphased between the starting compound $NiPS_3$ and a completely reduced phase Li_2NiPS_3,

$$x\ Li + Ni^{II}PS_3 \rightarrow x/2\ Li^{I}_2 Ni^{0} PS_3 + (1 - x/2)\ Ni^{II}PS_3.$$

We can observe that the $X1$ values (Fig. 3, solid circles) fit remarkably well with the solid line indicating that the nickel atoms reduced by lithium intercalation move from their initial octahedral sites to tetrahedral ones. This behavior, although unexpected if we consider previous results, is not really surprising since, in the literature (*16*), all the solid state chemistry examples of nickel in the oxidation state zero are found in the tetrahedral environment (only for complexes like $Ni(CO)_4$, $Ni(PF_3)_4$, $Ni(CNR)_4$).

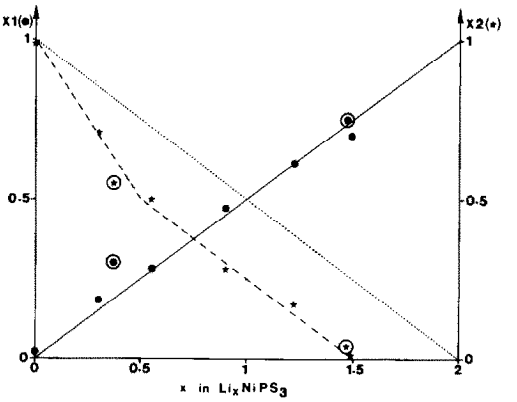

FIG. 3. Fitted fractions of nickel atoms in tetrahedral ($X1$) and octahedral ($X2$) sulfur sites. The solid line and the dotted line represent respectively the fraction of reduced and unreduced nickel atoms for the hypothesis of a regular reduction from the oxidation state two to zero. The broken line corresponds to another hypothesis with a slope (i) -1 for $x < 0.5$ and (ii) $-\frac{1}{2}$ for $x > 0.5$. The circled values correspond to the deintercalcated and reintercalated phases.

From the known structure of $NiPS_3$, the distance between the center of a tetrahedron and its corners can be estimated at 2.19 Å in the van der Waals gap and 2.15 Å in the slab. The nickel–sulfur fitted distance (2.28 Å) corresponds to a volume expansion of tetrahedral sites of about 15%. It is surprising that such a modification has never been detected on X-ray diffraction powder patterns. However, this may be compensated by an expected shrinking of the adjacent octahedron left by the migrant nickel.

If we consider now the $X2$ values on Fig. 3 (stars), it can be observed that they do not follow the dotted line, but are always situated below this theoretical line, corresponding to an apparent deficiency of nickel atoms in octahedral sites. Such a deficiency has no physical meaning, as EXAFS refers always to the environment of one atom, and must be explained either by an unsuited treatment of EXAFS spectra or a more complex structural situation.

The first hypothesis would correspond to a modification of the σ value for the nickel atoms in octahedral environment. An increase of the σ value in the sulfur octahedra, characteristic either of a site distortion or of a slight off-centered new position of nickel atoms, would result in a reduction of the corresponding EXAFS spectrum. As we chose to keep the Debye–Waller terms constant in the fits, such a reduction would give lower than expected values for the number of sulfur atoms. In order to test this hypothesis, new fits were performed varying all the parameters except γ. As pointed out above, this procedure gives rather erratic N and σ values, but a Debye–Waller term greater than 0.10 Å (value choosen for the first fits) has never been observed for all the series. Moreover, this hypothesis, which would correspond to a local modification of the starting phase, is not consistent with a biphased process.

To explain the apparent deficiency of

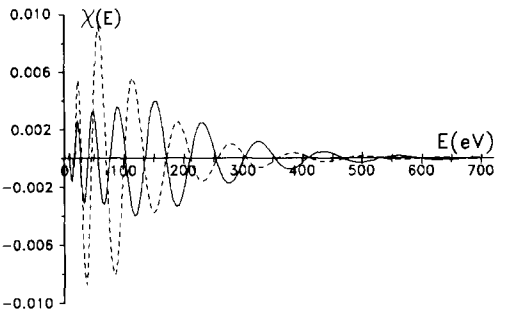

FIG. 4. Simulated EXAFS spectra for one sulfur atom (broken line) and one nickel atom (solid line) surrounding absorbing nickel at a distance of 2.46 Å.

nickel atoms in octahedral sites, the second possibility takes into account a first coordination shell of nickel atoms more complex than the one considered in the fits. Figure 4 shows, for example, that the EXAFS signals of sulfur and nickel backscatterers are almost in phase opposition, especially for $E > 200$ eV. If the displacement of the reduced nickel atoms is such as to form biatomic entities at a suitable distance, it would correspond to a strong decrease of the signal attributed to the nickel–sulfur octahedral environment. We will see later, in general structural considerations, that this environment may be probably still more complex.

The point corresponding to the $X1$ value of the deintercalated phase (Fig. 3) is situated slightly but significantly above the solid line indicating that, upon deintercalation, a part of reoxidized nickel atoms keep their tetrahedral environment. Thus the lithium intercalation process in $NiPS_3$ is not completely reversible and the formation of a "tetrahedral" phase could explain the forming process observed in the functioning of the lithium cells built with this material. The $X2$ value for this deintercalated phase is consistent with the one obtained at the first intercalation. At the same time, the results obtained for the richer intercalated phases ($x = 1.49$ and $x = 1.47$) at the first

and the second intercalation are very close. This fairly good reversibility confirms definitely that the thiophosphate is not destroyed by lithium intercalation.

In Fig. 5, $Y1$ and $Y2$ values extracted from Table II can be compared with the theoretical line of slope $-\frac{1}{2}$ which represents, in the above intercalation reaction, the number of unreduced nickel atoms. The good fit between the calculated values and the theoretical line shows that the reduced nickel atoms, in their new position, have no more atoms at the initial distances, namely in the 3.30–3.60 Å range. This result allows the conclusion that the nickel migration takes place in the slab and not in the van der Waals gap. In effect, in this last hypothesis, the nickel atoms would have, as second neighbors, one phosphorus atom at 3.29 Å and three phosphorus atoms at 3.69 Å. The regular decrease of $Y2$ (number of phosphorus atoms divided by six) following a $1 - x/2$ law rules out such an hypothesis. The $Y1$ and $Y2$ values of deintercalated and reintercalated phases are in agreement with those obtained in the first intercalation except $Y1$ for the deintercalated compound. Its low value is consistent with the above consideration where a part of reoxidized nickel atoms keep their tetrahedral environment and do not contribute to the second coordination shell as they were doing in the starting compound.

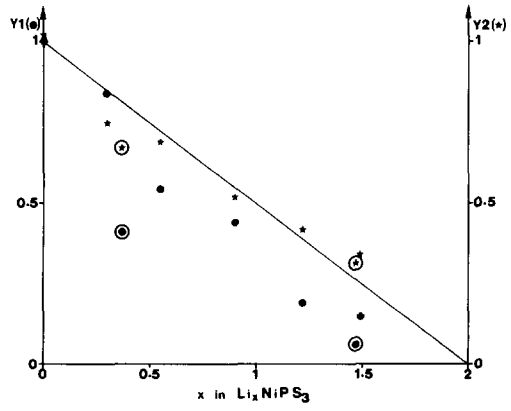

FIG. 5. Fitted fraction of nickel atoms keeping the initial second coordination shell calculated either from the numer of atoms of nickel ($Y1$) or phosphorus ($Y2$). The solid line represents the number of unreduced nickel atoms in the first hypothesis. The circled values correpond to the deintercalated and reintercalated phases.

B. Global Structure of the Intercalated Phase(s)

From the EXAFS study, we can conclude undoubtedly that when lithium is intercalated in the lamellar structure of $NiPS_3$, the reduced nickel atoms move from their initial octahedral sites to tetrahedral ones in the slab. From this new and unexpected result, it is interesting to reinvestigate the previous results obtained by magnetic susceptibility measurements and ^{31}P NMR spectroscopy to try to determine and explain the structural and electronic nature of the reduced materials. Considering that the lithium can be put in $NiPS_3$ and taken out, we may assume that the initial structure of $NiPS_3$ is globally maintained but locally modified by the intercalated lithium and the motions of the nickel atoms. In other words we assume that the $(P_2S_6)^{4-}$ arrangement which characterizes the compound framework remains the same. The ^{31}P NMR experiments (*6*) detect, only for lithium content greater than 0.5 mole per mole of $NiPS_3$, the occurrence of a diamagnetic phase that can be explained by the occurrence of atoms at the oxidation state zero. At the same time, the magnetic susceptibility measurements (*17*) confirm this hypothesis through the observation of a regular decrease of the room temperature susceptibility. These results led us in particular to determine the formation of the completely reduced intercalated phase Li_2NiPS_3, but asked the question of the redox process at the beginning of the intercalation ($0 < x < 0.5$ for which no apparent change is seen on ^{31}P NMR spectra).

A projection of a $NiPS_3$ slab structure

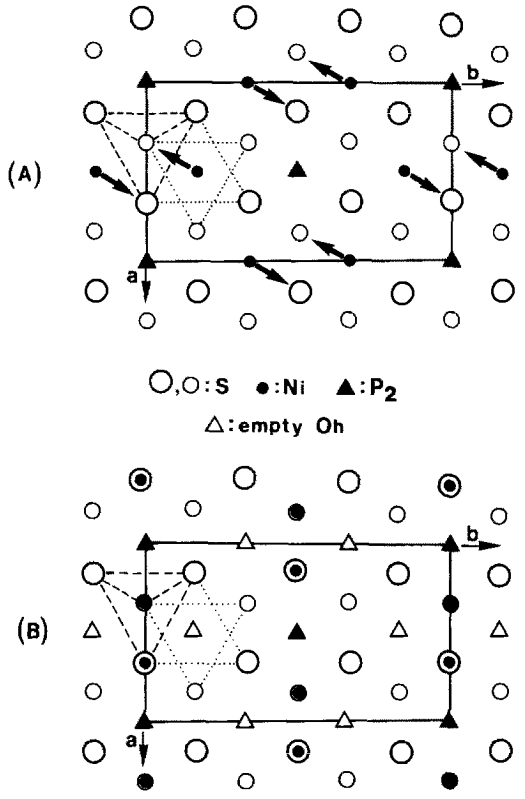

FIG. 6. (A) Projection of a slab perpendicularly to the *ab* plane in the monoclinic cell of $NiPS_3$. The arrows indicate a possible migration for the reduced nickel atoms. (B) Hypothetical structure of the completely reduced Li_2NiPS_3 phase resulting from the migration of A.

perpendicularly to the *ab* monoclinic plane is represented in Fig. 6A. A given nickel atom in an octahedral site has six adjacent tetrahedra in the slab for a possible migration. We can observe that all these tetrahedra are also adjacent to an octahedron containing a phosphorus–phosphorus pair. Thus, when nickel moves into a tetrahedron, it comes closer to the phosphorus atoms. Calculations performed for an unmodified $NiPS_3$ anionic structure give nickel–phosphorus distances of 1.95 and 2.55 Å. Therefore it is very important to note that the first coordination shell contains at least four different atoms. It is well known that it is impossible to fit EXAFS spectra with so many parameters. Furthermore, it is very difficult to similate the influence of these phosphorus atoms, as the actual nickel–phosphorus distances are not known. Nevertheless it is possible to put forward two main different hypotheses for the structure of the reduced phase(s).

The first one takes into account a regular increasing deficiency of $X2$ values as compared to the theoretical dotted line in Fig. 3. Such a variation can be explained by the occurrence of biatomic nickel–nickel entities when nickel atoms move in tetrahedral sites. In effect, in a perfectly regular compact stacking, the distance between the center of an octahedron and its corners is exactly equal to the distance between the centers of two adjacent tetrahedra. As seen above (Fig. 4), the nickel and sulfur backscattering phases are almost exactly in phase opposition and the occupation, by reduced nickel atoms, of adjacent tetrahedra, sharing an edge, gives nickel–nickel distances equal to nickel–sulfur distance in octahedra in $NiPS_3$. The formation of such groups explains well the apparent deficiency of the proportion of nickel atoms in octahedra and its increase with lithium content. This hyphothesis sustains a biphased reduction process between the starting compound $NiPS_3$ and the completely reduced phase Li_2NiPS_3 where nickel atoms, at the oxidation state zero, occupy, two by two, adjacent tetrahedra. It must be mentioned that the formation of such biatomic entities is sustained by the variation of the number of nickel atoms surrounding absorbing nickel in the second coordination shell. In effect, we have seen that all the reduced nickel atoms have lost all neighbors at a distance of about 3.4 Å and it is impossible for these atoms to occupy the tetrahedra in the gap at distances very different of 3.4 Å without forming biatomic groups. Figure 6A shows a possible coordi-

nated migration of nickel atoms (arrows) and the hypothetical resulting structure of the Li_2NiPS_3 phase is represented on Fig. 6B. This hypothetical structure maintains the initial frame of $NiPS_3$ with the space group $C2/m$ explaining why no extra diffraction lines appear in powder X-ray diffraction experiments. It corresponds to the formation of cationic lines along the a parameter with successively a P_2 pair in an octahedron, two Ni atoms in two adjacent tetrahedra, one P_2 pair in an octahedron, and so on. Theoretical X-ray powder diffraction patterns were calculated using the Lazy pulverix program (*18*) for this hypothetical structure and others where Ni atoms occupy always two by two adjacent tetrahedra in the slab. These patterns differ largely from one hypothesis to another one and show always large modifications versus the $NiPS_3$ one (occurrence for example of a line around $d = 5$ Å corresponding to 020 or 110 indices). As stated above, such modifications have never been observed. This phenomenon probably is to be related to the microbiphased intercalation process with grain size lower than the X-ray diffraction correlation length. In effect, ESR measurements performed on the parent compound $FePS_3$ (*19*) allowed the estimation of the number of unit cells containing the reduced transition metal. Twenty-five and 200 cells were found respectively for $x = 0.5$ and $x = 1.1$.

Octahedral empty sites, previously occupied by Ni atoms, are available for an occupation by intercalated lithium atoms, or their migration. This intercalation scheme is not completely satisfactory as it does not explain why the NMR and magnetic susceptibility measurements detect the diamagnetic phase only for lithium content greater than 0.5 instead of a continuous process from the very beginning as suggested by the EXAFS results.

The second hypothesis is based on a slightly different variation of $X2$, following, for $x < 0.5$, a law in $-x$ and, for $x > 0.5$, a law in $-x/2$ (represented by the broken line on Fig. 3). Such a variation, with a break for the composition $Li_{0.5}NiPS_3$, is very satisfactory if compared with the NMR and magnetic susceptibility results. It supposes that the intercalation process is monophased for $x < 0.5$ and, after this composition, biphased between $Li_{0.5}NiPS_3$ and Li_2NiPS_3 phases (although this latter cannot be reached for the whole sample). As mentioned above, the results obtained for the second coordination shell evidence the formation of biatomic nickel entities, confirming the final term of the intercalation: Li_2NiPS_3. The main difference concerns the beginning of the intercalation, where a phase, containing nickel atoms in tetrahedral and octahedral sites, must be considered. In such a phase, the distance between a given nickel atom in a tetrahedron and another one in an adjacent octahedron is exactly equal to the nickel–sulfur distance in a tetrahedron NiS_4, as far as a perfect compact stacking is considered. The above argument about the nickel and sulfur backscattering phases led us to consider a deficit in the number of nickel atoms in tetrahedral sites. The variation of $X1$ in $x/2$ would be an accident and would correspond in fact to a variation in x reduced by adjacent position of reduced nickel atoms in tetrahedra and the others in octahedra. The intermediate phase $Li_{0.5}NiPS_3$ would then correspond to the following reduction process (for $x < 0.5$),

$$x\ \mathrm{Li} + \mathrm{Ni^{II}PS3} \rightarrow \mathrm{Li^{I}_{x}Ni^{I}_{x}Ni^{II}_{1-x}PS_3},$$

in order to fit with the observed variation of the proportion of nickel atoms in octahedral environment following a law in $1 - x$. This intercalated phase where nickel is reduced at the oxidation state I is not diamagnetic and can explain why no diamagnetic phase has been detected before the composition $Li_{0.5}NiPS_3$. From a structural point of view, this process agrees well with the supposed

early lithium intercalation in 2*d* octahedral sites of the van der Waals gap. These sites are ordered and are completely full at the composition $Li_{0.5}NiPS_3$. For lithium content greater than 0.5 the Ni_{Td}–Ni_{Oh} groups would progressively disappear to the benefit of Ni_{Td}–Ni_{Td} ones, corresponding then to an apparent deficit of nickel atoms in the octahedra. This second hypothesis fits better than the first one with the previous physical measurements but it supposes that the so nice variation of $X1$ following a law in $x/2$ is in fact an accident.

It is impossible to explain completely the intercalation process by this EXAFS study. In effect, mainly depending on the variation of $X1$ and $X2$ versus x in Li_xNiPS_3, two hypotheses can be supported. The values of $N1$ and $N2$, which give $X1$ and $X2$, were fitted very carefully but it is well known that their accuracy is usually not very good. Moreover, in order to confirm, or not, the break at $x = 0.5$, which makes the difference between the two hypotheses, it would be interesting to perform the EXAFS study for a greater number of different compositions. In the same manner, a study of a wide range of deintercalated phases would be very fruitful. It is however difficult to prepare chemically a great number of different phases, especially the deintercalated one, for different intercalation ratios. That is the reason why we have undertaken the design of an electrochemical cell on which EXAFS spectroscopy could be performed *in situ*. It could then be possible to obtain very quickly, on the same sample, many accurate compositions for either intercalated or deintercalated samples and not only at the first cycle.

V. Conclusion

The EXAFS study of lithium-intercalated phases of the lamellar thiophosphate $NiPS_3$ gave a new insight on the intercalation process. A structural rearrangement has been observed during this reaction, corresponding to a migration of the reduced nickel atoms from their initial octahedral sulfur sites to tetrahedral ones in the slab. This behavior may explain the forming observed in cycling the electrochemical cells using this intercalation and may be thought to participate to the gradual amorphization of the thiophosphate. This correponds to the formation of a new phase $NiPS_3$ containing a fraction of nickel atoms tetrahedrally coordinated. Such a phase can be related to the amorphous form a-$NiPS_3$ (*20*), obtained by a coprecipitation reaction at room temperature, where some nickel atoms may occupy tetrahedral sites.

Unfortunately, it is impossible from this study to describe completely the lithium intercalation process in $NiPS_3$, taking into account the previous physical results. The observed nickel motion must induce some modifications in the intensities of the X-ray diffraction lines. A structural study is currently underway to determine the nature of such changes. In order to ensure precision of the above results, an EXAFS study will be performed *in situ* in an electrochemical cell, expecting to obtain a large number of compositions in the Li_xNiPS_3 system either at the intercalation or the deintercalation stage.

Acknowledgments

We thank Y. Chabre for very helpful discussions and ECC for financial support under Contract ST2P 0013-3F.

References

1. (a) W. Klingen, G. Eulenberger, and H. Hahn, *Z. Anorg. Allg. Chem.* **401,** 97 (1973). (b) G. Ouvrard, R. Brec, and J. Rouxel, *Mater. Res. Bull.* **20,** 1181 (1985).
2. A. H. Thompson and M. S. Whittingham, *Mater. Res. Bull.* **12,** 741 (1977).
3. A. Le Mehaute, G. Ouvrard, R. Brec, and J. Rouxel, *Mater. Res. Bull.* **12,** 1191 (1977).

4. A. DE GUIBERT AND A. HERMELIN, *J. Power Sources* **14,** 57 (1985).
5. G. OUVRARD, Thesis, Nantes, France (1980).
6. Y. CHABRE, P. SEGRANSAN, C. BERTHIER, AND G. OUVRARD, *in* "Fast Ion Transport in Solids" (P. Vashishta, J. N. Mundy, and G. K. Shenoy, Eds.), p. 221, North-Holland, Amsterdam (1979).
7. G. A. FATSEAS, M. EVAIN, G. OUVRARD, R. BREC, AND M. H. WHANGBO, *Phys. Rev. B* **35,** 3082 (1987).
8. M. H. WHANGBO, R. BREC, G. OUVRARD, AND J. ROUXEL, *Inorg. Chem.* **24,** 2459 (1985).
9. Y. MATHEY, A. MICHALOWICZ, P. TOFFOLI, AND G. VLAIC, *Inorg. Chem.* **23,** 897 (1984).
10. Y. MATHEY, H. MERCIER, AND A. MICHALOWICZ, *J. Phys. C* **8,** 875 (1986).
11. G. OUVRARD, *Mater. Sci. Eng. B* **3,** 81 (1989).
12. M. B. DINES, *Mater. Res. Bull.* **10,** 287 (1975).
13. B. K. TEO AND P. A. LEE, *J. Amer. Chem. Soc.* **101,** 2815 (1979).
14. E. PROUZET, G. OUVRARD, R. BREC, S. BENAZETH, AND H. DEXPERT. *J. Chim. Phys. B* **6,** 1675 (1989).
15. S. A. SUNSHINE AND J. A. IBERS, *Inorg. Chem.* **24,** 3611 (1985).
16. A. F. WELLS, "Structural Inorganic Chemistry," 5th ed., p. 1231, Clarendon Press, Oxford (1984).
17. R. BREC, *Solid State Ionics* **22,** 3 (1986).
18. R. YVON, W. JEITSCHKO, AND E. PARTHE, *J. Appl. Crystallogr.* **10,** 73 (1977).
19. P. COLOMBET, G. OUVRARD, O. ANTSON, AND R. BREC, *J. Magn. Magn. Mater.* **71,** 100 (1987).
20. E. PROUZET, G. OUVRARD, AND R. BREC, *Solid State Ionics* **31,** 79 (1988).